

# Theoretical model to determine the effects of geometrical factors on the resorption of calcium phosphate bone substitutes

M. Böhner<sup>a,\*</sup>, F. Baumgart<sup>b</sup>

<sup>a</sup>*Dr. Robert Mathys Foundation, Bischmattstrasse 12, 2544 Bettlach, Switzerland*

<sup>b</sup>*AO Technical Commission, Clavadelerstrasse, CH-7270 Davos Platz, Switzerland*

Received 29 September 2003; accepted 9 October 2003

## Abstract

A theoretical approach was used to determine the effect of geometrical factors on the resorption rate of calcium phosphate bone substitutes that are either dense, microporous, and/or contain spherical macropores. Two cases were considered: (a) macroporous blocks that can be invaded by resorbing cells either directly because the structure is fully open-porous, or indirectly after some resorption of the macropores walls and/or interconnections. (b) Microporous or dense blocks/granules that cannot be invaded by resorbing cells, i.e. can only be resorbed from the outside to the inside, layer by layer. The theoretical approach was based on five assumptions: (i) the pores are spherical; (ii) the pores are ordered according to a face-centered cubic packing; (iii) the resorption is surface-controlled; (iv) the resorption is only possible if the surface can be accessed by blood vessels of 50  $\mu\text{m}$  in diameter; and (v) the resorption time of a given amount of calcium phosphate is proportional to the net amount of material. Based on these assumptions, the calculations showed that the resorption time of a macroporous block could be minimized at a specific pore radius. This pore radius depended (i) on the size of the bone substitute and (ii) on the interpore distance. Typical radii were in the range of 100–400  $\mu\text{m}$ . These values are similar to the numerous pore size optima mentioned in the scientific literature. For microporous or dense blocks/granules, the model suggested that a relatively small radius should be preferred. Such a radius leads to an optimum combination of a high surface area favorizing resorption and the presence of large intergranular gaps favorizing blood vessel ingrowth. In that case, the optimum of granule radius is around 100–200  $\mu\text{m}$ . Finally, a very good agreement was found between the predictions of the model and experimental data, i.e. the model explained in all but two cases the results with an accuracy superior to 80%. In conclusion, the model appears to be a useful tool to better understand *in vivo* results, and possibly better define the geometry and distribution of the pores as well as the size of a bone substitute.

© 2003 Elsevier Ltd. All rights reserved.

**Keywords:** Pore; Resorption; Size; Calcium phosphate; Ceramic; Model

## 1. Introduction

Calcium phosphate ceramics have proved their adequacy and efficiency as bone substitute materials [1]. Despite their widespread use, there is a growing demand for faster resorbable calcium phosphate bone substitutes. The resorption rate of a bone substitute depends on many factors such as the patient (sex, age, metabolism, social habits, etc.), the implant location, the composition of the bone substitute and its geometry. For a surgeon or an engineer, it is difficult to control the first factors, but possible to control the composition and

geometry of the bone substitute. In the last two decades, new compositions have been proposed such as dicalcium phosphate dihydrate [2,3], octocalcium phosphate [4,5],  $\alpha$ -tricalcium phosphate [6], or calcium pyrophosphate [7]. However, very little work has been done to investigate the effect of geometry on the resorption rate of bone substitutes. The main reason is that it is difficult to synthesize calcium phosphates with specific geometrical features. In particular, it is difficult to vary one parameter, e.g. the macroporosity, without varying other parameters, e.g. the microporosity or the size of the pore interconnections. Here, a different approach is proposed, i.e. a theoretical model is used to predict the effect of geometry on the resorption rate of bone substitutes. The model is devoted to bone substitutes that are either dense, microporous, and/or contain

\*Corresponding author. Tel.: +41-32-6441413; fax: +41-32-6441176.

E-mail address: [marc.bohner@rms-foundation.ch](mailto:marc.bohner@rms-foundation.ch) (M. Böhner).

Nomenclature		
$r_p$	pore radius	$th_{r,tot}$ total resorbed thickness (resorption)
$d_p$	distance between the pores (from wall to wall)	$S_p$ pore surface
$d_{octgap}$	largest distance between two neighboring pores	SA surface area per unit volume
$r_i$	radius of the interconnection	$p$ porosity
$r_{g,0}$	initial granule radius	$V_c$ volume of a face-centered cube
$r_{cyl,0}$	initial cylinder radius	$V$ volume of a partially full sphere
$h_{cyl,0}$	initial cylinder height	$V_p$ volume of a pore
$l_{prism,0}$	initial length of the rectangular prism	$V_i$ volume of a pore interconnection
$w_{prism,0}$	initial width of the rectangular prism	$V_{g,0}$ initial granule volume
$h_{prism,0}$	initial height of the rectangular prism	$V_{g,t}$ granule volume at time “ $t$ ”
$y$	unfilled height of a sphere	$V_{cyl,0}$ initial volume of a cylinder
$W$	Width of a block	$V_{cyl,t}$ volume of a cylinder at time “ $t$ ”
$th_i$	resorbed thickness (bone ingrowth)	$V_{prism,0}$ initial volume of a rectangular prism
$th_r$	resorbed thickness (resorption)	$V_{prism,t}$ volume of a rectangular prism at time “ $t$ ”
$th_{i,tot}$	total resorbed thickness (bone ingrowth)	$t$ time
		$R_R$ linear resorption rate

spherical macropores. The theoretical predictions are then compared to the experimental results presented in the literature. Finally, conclusions are drawn on the adequacy of the model and its usefulness in predicting in vivo results and designing faster resorbable bone substitutes.

Two separate cases are considered in the present study: (i) macroporous blocks, i.e. blocks that can be invaded by cells; and (ii) microporous blocks and granules that cannot be invaded by cells. In the first category, resorption can occur throughout the sample provided cells can invade it. Cell migration into the block can be direct, i.e. without any ceramic resorption, or indirect, i.e. after partial resorption of the macropore walls until a given interconnection size is reached. In the second category, resorption can only occur on the outer surface because micropores are too small to enable cell invasion. As a result, a resorbing cell (e.g. osteoclast, macrophage) sees two types of surfaces: (i) a surface full of pores that can be denominated as “concave bone substitute” and (ii) a closed surface, denominated here “convex bone substitute”.

The theoretical approach was based on five assumptions: (i) the pores are spherical; (ii) the pores are ordered according to a face-centered cubic packing; (iii) the resorption is surface-controlled; (iv) the resorption is only possible if the surface can be accessed by blood vessels of 50  $\mu\text{m}$  in diameter; and (v) the resorption time of a given amount of calcium phosphate is proportional to the net amount of material. The adequacy of these assumptions and their influence on the theoretical predictions is discussed hereafter (Section 2.4).

In the present study, concave bone substitutes are assumed to contain pores that are homogeneously distributed according to a cubic face-centered (CFC) packing (Fig. 1). In this type of structure, a pore is

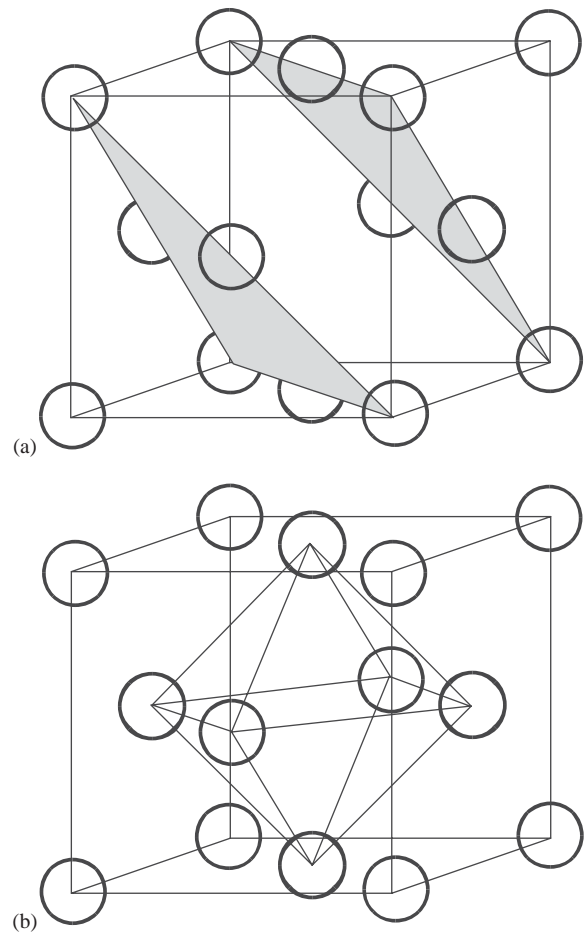


Fig. 1. CFC lattice showing (a) the layers of pores and (b) the octahedral gap between the pores.

present at each corner of the cube, as well as at each center of a face of the cube. The radius,  $r_p$ , of the pores and the distance,  $d_p$ , between pores are the most

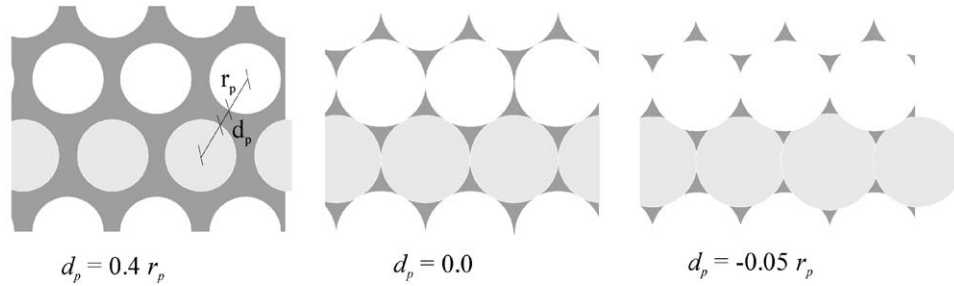


Fig. 2. Three examples of a face-centered cubic packing. The distance between pores varies from  $d_p = 0.4r_p$  to  $-0.05r_p$ .

important geometrical entities describing the porous structure (Fig. 2).

**2. Theoretical**

Theoretical considerations are first made for concave bone substitutes and then for convex bone substitutes.

*2.1. Concave bone substitutes*

*2.1.1. Porosity*

Assuming that the pores have a CFC packing (Fig. 1), each cube contains  $6 \times 0.5 + 8 \times 0.125 = 4$  pores. The cube has the following volume,  $V_c$  (Fig. 3):

$$V_c = \left( \frac{(4r_p + 2d_p)}{\sqrt{2}} \right)^3 \tag{1}$$

The porosity is

$$p = \frac{4V_p}{V_c} \tag{2}$$

where  $V_p$  is the volume of each pore. If  $d_p > 0$ , the volume of each pore is

$$V_p = \frac{4}{3} \pi r_p^3 \tag{3}$$

and the porosity becomes

$$p = \frac{16(2)^{3/2} \pi r_p^3}{3(4r_p + 2d_p)^3} = \frac{4\sqrt{2} \pi r_p^3}{3(2r_p + d_p)^3} \quad (d_p > 0). \tag{4}$$

If  $d_p = 0$ , the porosity is equal to 0.740 which is the maximum packing density of unisized spheres.

If  $d_p < 0$ , the calculation of the porosity is slightly more complicated because each pore is superimposed with 12 neighboring pores. The volume of each interconnection can be calculated knowing that the volume,  $V$ , of a partially full sphere is given by (Fig. 4)

$$V = \int_0^y \pi(r_p^2 - (r_p - z)^2) dz = \frac{\pi}{3} y^2(3r_p - y). \tag{5}$$

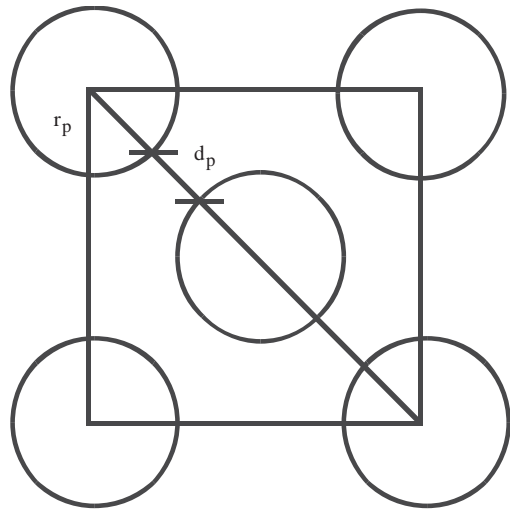


Fig. 3. CFC packing of pores. Here, one face of the cube is represented.

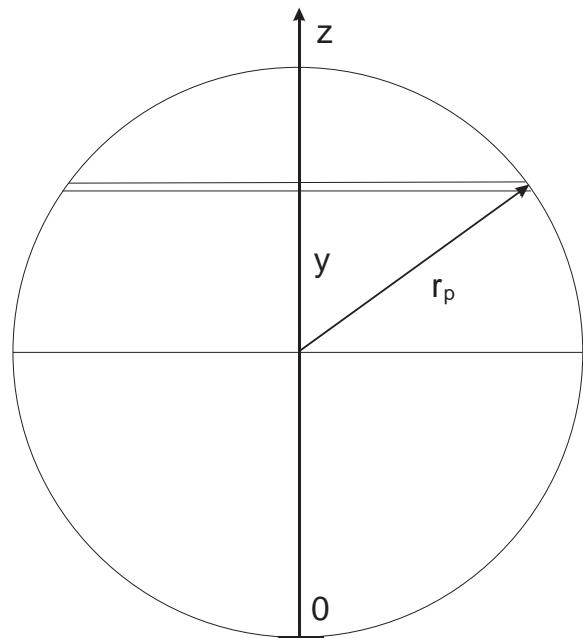


Fig. 4. Pore filled up to a height  $y$ . Volume of a slice:  $\pi(r_p - (r_p - z))^2 dz$ .

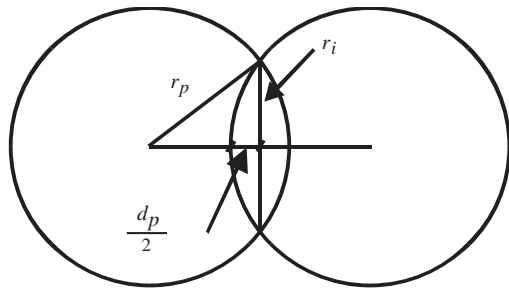


Fig. 5. Two interconnected pores showing the pore radius,  $r_p$ , the radius of the interconnection,  $r_i$ , and the distance between the pores,  $d_p$  ( $d_p < 0$ ).

As a result, the volume,  $V_i$ , of each interconnection is given by

$$V_i = \frac{4}{3} \pi r_p^3 - \frac{\pi}{3} y^2 (3r_p - y). \quad (6)$$

In the present model,  $y$  is equal to (Fig. 5)

$$y = 2r_p + \frac{d_p}{2}. \quad (7)$$

The combination of Eqs. (6) and (7) gives

$$V_i = \frac{\pi}{4} d_p^2 \left( r_p + \frac{d_p}{6} \right). \quad (8)$$

So, the volume of each pore,  $V_p$ , is given by

$$V_p = \frac{4}{3} \pi r_p^3 - 12V_i = \frac{4}{3} \pi r_p^3 - \pi d_p^2 \left( 3r_p + \frac{d_p}{2} \right). \quad (9)$$

Combining Eqs. (1), (2) and (9) gives the porosity

$$p = \frac{\frac{16}{3}(2)^{3/2} \pi r_p^3 - 4(2)^{3/2} \pi d_p^2 (3r_p + (d_p/2))}{(4r_p + 2d_p)^3} \\ = \pi \sqrt{2} \frac{8r_p^3 - 18r_p d_p^2 - 3d_p^3}{6(2r_p + d_p)^3} \quad (d_p < 0). \quad (10)$$

Eq. (10) is only valid when the absolute value of  $d_p$  is small. When the latter value increases, more than two pores can be simultaneously superimposed. This condition corresponds to  $d_p = -0.268r$  (see hereafter).

The effect of the distance between pores,  $d_p$ , on the pore structure and porosity is represented in Figs. 2 and 6. These results show that a very small variation of  $d_p$  can have a very large effect on the pore structure, and in particular on the pore interconnections.

### 2.1.2. Pore interconnection

In the present model pore interconnections can only exist when the distance between pores,  $d_p$ , is negative. In that case, the size of the pore interconnections,  $r_i$ , can be expressed as a function of the pore radius,  $r_p$ , and the distance between pores,  $d_p$  (Fig. 5)

$$r_p^2 - \left( r_p + \frac{d_p}{2} \right)^2 = r_i^2, \quad (11)$$

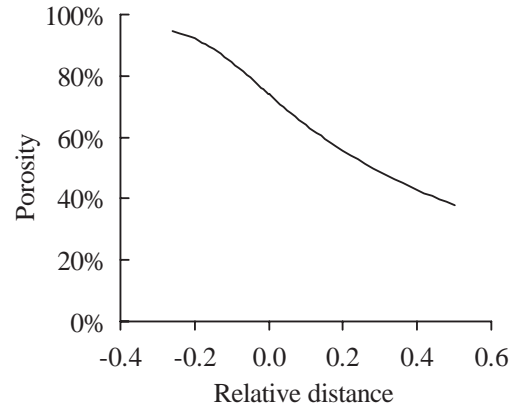


Fig. 6. Effect of the interpore distance  $d_p$  on the porosity of the bone substitute. In the chart, the interpore distance corresponds to the ratio  $d_p/r_p$ .

$$r_i = \frac{\sqrt{(-d_p(4r_p + d_p))}}{2}. \quad (12)$$

If  $r_i > 0.5r_p$ , more than two pores are simultaneously superimposed in one location. This condition corresponds to

$$d_p < -r_p(2 - \sqrt{3}) = -0.268r_p. \quad (13)$$

The corresponding porosity is 96.4%. In this article, calculations are restricted to value of,  $r_i < 0.5r_p$ , since calcium phosphate bone substitutes consisting of more than 85–90% porosity would be too brittle to be used.

### 2.1.3. Bone ingrowth

Recently, Lu et al. [8] showed that an optimal resorption can only be achieved if the pore interconnections have a diameter larger than 50  $\mu\text{m}$ . In the present model, this requirement can only be achieved if the distance between the pores,  $d_p$ , is negative enough (all distances in micrometers; see Eq. (12))

$$d_p < -2 \left( r_p - \sqrt{r_p^2 - r_i^2} \right), \quad (14)$$

where  $r_i = 25 \mu\text{m}$  (it is assumed that this value is a constant throughout the whole document). Obviously, this requirement can only be fulfilled if the pore radius,  $r_p$ , is larger than 25  $\mu\text{m}$ . Moreover, this condition implies that the porosity is larger than 74% (Fig. 7). Interestingly, the minimum porosity depends on the pore size: the larger the pore size is, the lower the minimum porosity must be. If the porosity of the structure is lower than this minimum value, the pores are either not interconnected or the interconnections are too small for blood vessels to invade the structure and enable resorption to take place and bone to grow in. In that case, resorption takes place in steps: the first pore interconnections have to be created and/or enlarged before bone can grow in and enlarge the next pore interconnections, and so on (Fig. 8). The thickness,  $th_i$ ,

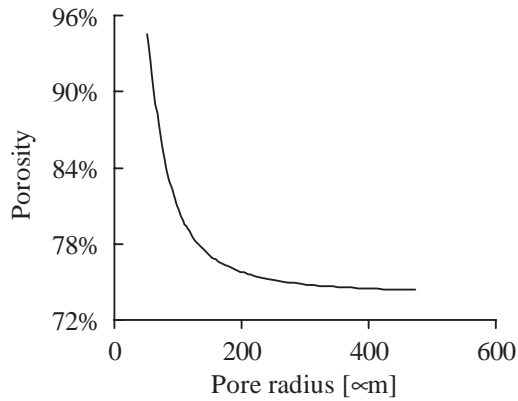


Fig. 7. Minimum porosity required to have an open-porous structure with an interconnection diameter ( $= 2r_i$ ) larger than  $50 \mu\text{m}$ .

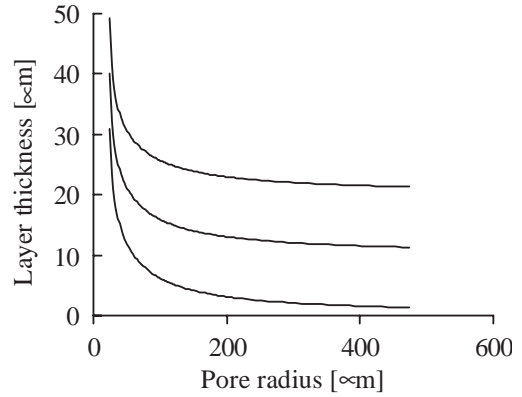


Fig. 9. Layer thickness,  $th_i$ , that has to be resorbed to enable bone ingrowth.  $r_i = 25 \mu\text{m}$ . Top curve:  $d_p = 20 \mu\text{m}$ ; Middle curve:  $d_p = 10 \mu\text{m}$ ; Bottom curve:  $d_p = 0 \mu\text{m}$ .

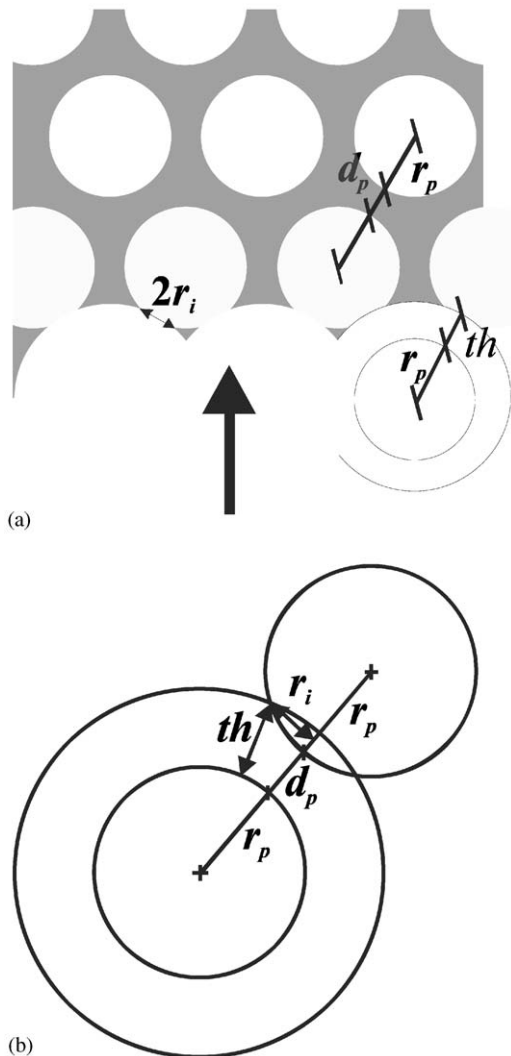


Fig. 8. Resorption of a porous block row by row. The large circle represent a pore that has been enlarged by resorption. The distance by which the pore has been enlarged is the distance  $th_i$ . The direction of the arrow indicates the direction of the resorption. (a) Overview; (b) details.

of the ceramic layer that has to be resorbed to open the pores to enable the ingrowth of blood vessel can be calculated using simple geometrical rules

$$2r_p + d_p = \sqrt{r_p^2 - r_i^2} + \sqrt{(r_p + th_i)^2 - r_i^2}$$

$$\text{for } d_p > -2\left(r_p - \sqrt{r_p^2 - r_i^2}\right).$$
(15)

Therefore,

$$th_i = \sqrt{r_i^2 + (2r_p + d_p - \sqrt{r_p^2 - r_i^2})^2} - r_p$$

$$\text{for } d_p > -2\left(r_p - \sqrt{r_p^2 - r_i^2}\right),$$
(16)

where  $r_i = 25 \mu\text{m}$ . The results show that the thickness grows very rapidly with a decrease of the pore size (keeping  $d_p = 0$ ; Fig. 9). This effect is even more striking when the thickness is related to the pore radius (Fig. 10): for pores smaller than  $r_i (= 25 \mu\text{m})$ , the layer thickness that has to be removed to enable blood vessel ingrowth is larger than the pore radius itself. In fact, when  $r_p < r_i$ , the only way to have resorption is to proceed layer by layer, which means that the resorption is very slow. Therefore, the importance of the presence of pore interconnections increases with a decrease of the pore size.

#### 2.1.4. Resorption rate

In the preceding paragraphs, calculations were done to assess how fast blood vessels and bone cells can invade a porous structure depending on the pore size and interconnection. It is clear that the rate at which bone ingrowth occurs has an influence on the resorption rate. However, this is certainly not the only factor. If two structures can be fully invaded by osteoclasts, the resorption rate must depend on the interface between bone and ceramic, i.e. on the surface area of the pores.

To estimate the change of surface with the extent of resorption, the total surface area of a block should be

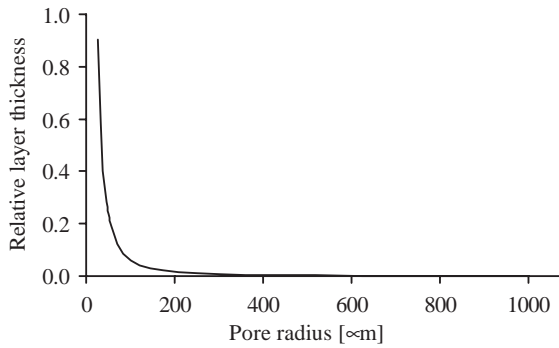


Fig. 10. Relative layer thickness that has to be resorbed to enable bone ingrowth.  $d_p = 0 \mu\text{m}$ . The relative layer thickness corresponds to the ratio between the layer thickness and the pore radius.  $r_i = 25 \mu\text{m}$ .

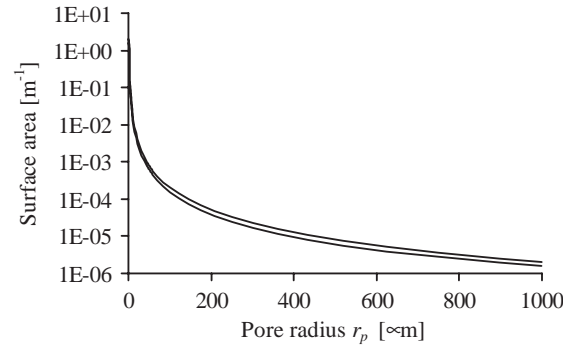


Fig. 11. Surface area of a porous block as a function of the pore radius,  $r_p$ . The distance between pores,  $d_p$ , is: lower curve:  $-0.15r_p$ ; upper curve:  $-0.05r_p$ .

expressed as a function of the pore radius and the distance,  $th_r$ , of material that has been resorbed. The surface area of one pore,  $S_p$ , is the surface of the pore without interconnections minus the surface area of each 12 interconnections

$$S_p = 4\pi r_p^2 - (-12\pi r_p d_p) = 4\pi r_p^2 + 12\pi r_p d_p \quad (d_p < 0). \quad (17)$$

This relationship is only valid for small  $d_p$  values (see Eq. (13)). In Eq. (17), the surface area increases with an increase of pore radius. However, bigger pores take more space. Therefore, this equation should be calculated per unit volume. Previously, it was shown that each cube unit contained 4 pores and had the volume given by Eq. (1). Therefore, the surface area per unit volume, SA, is obtained by combining Eqs. (1) and (17):

$$SA = 4 \frac{S_p}{V_c} = 4\sqrt{2}\pi r_p \frac{(r_p + 3d_p)}{(2r_p + d_p)^3}. \quad (18)$$

As a result, the surface area decreases almost exponentially with an increase of pore size (Fig. 11). Obviously, if a small layer of material is removed on all surfaces, the relative decrease of surface area must be much larger for a small pore size. To calculate this, the pore radius and interpore distance of Eq. (18) must be replaced by

$$r_p \Leftrightarrow r_p + th_r, \quad (19)$$

$$d_p \Leftrightarrow d_p - 2th_r, \quad (20)$$

where  $th_r$  is the thickness of the resorbed layer. For example, when  $th_r = 0.05 \mu\text{m}$ , the porosity is strongly increased at a low pore radius ( $r_p < 20 \mu\text{m}$ ), but not modified at a large pore radius (Fig. 12). This result indicates that the resorption rate of a porous surface is almost inversely proportional to the pore size, but only if the surface is accessible, i.e.  $r_i > 25 \mu\text{m}$ .

As previously seen, two factors play a role to estimate the optimal pore diameter: how fast bone cells can invade the implant in order to start resorbing it, and how fast one unit cell can be resorbed. It was shown that

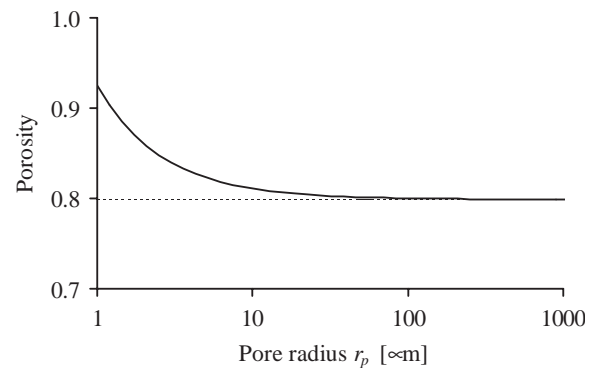


Fig. 12. Porosity as a function of pore radius for  $d_p = -0.05r_p$  and  $th = 0.00 \mu\text{m}$  (bottom curve);  $th = 0.05 \mu\text{m}$  (top curve).

an increase in pore size eases bone ingrowth and a decrease of pore size accelerates the resorption of a unit cell. Therefore, there must be a pore size optimum which must depend not only on porous structure of the bone substitute (Eq. (16)), but also on its size. Indeed, a larger block has more pores which require a larger number of pore openings. In the CFC packing, when two pores are opened by resorption, cells can move by a linear distance of  $4r_p + 2d_p$  (Fig. 2). Therefore, if the width of a block is  $W$ , the total distance that has to be resorbed to allow bone ingrowth within the block,  $th_{i,tot}$ , is given by (assuming that bone ingrowth occurs from both sides of the block and that bone ingrowth is perpendicular to the implant surface)

$$th_{i,tot} = \frac{2th_i}{4r_p + 2d_p} \frac{W}{2} = \frac{\sqrt{r_i^2 + (2r_p + d_p - \sqrt{r_p^2 - r_i^2})^2} - r_p}{4r_p + 2d_p} W \quad (21)$$

for  $d_p > -2(r_p - \sqrt{r_p^2 - r_i^2})$ .

This total layer thickness decreases very rapidly with an increase of the pore radius (Fig. 13). The layer

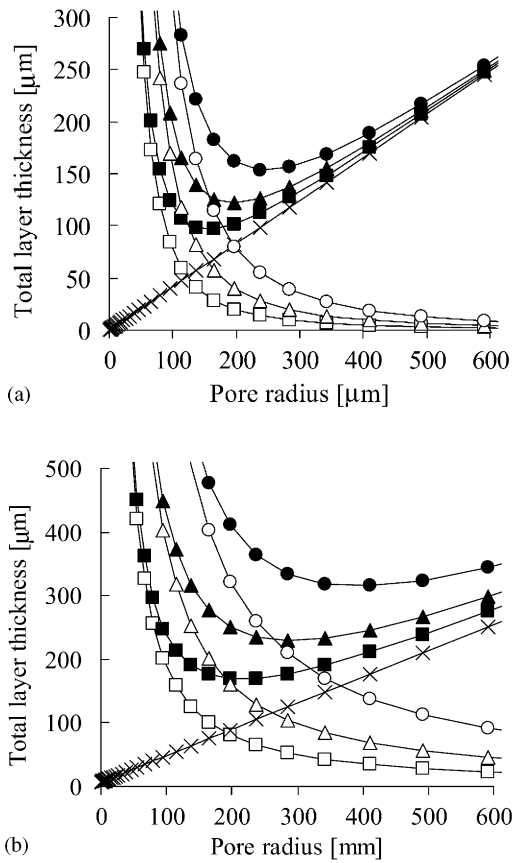


Fig. 13. Total layer thickness that has to be resorbed in order to (x) fully resorb one unit cell of the block or to (Δ, ○, □) open all the pores of the block to enable bone ingrowth. Conditions: (a)  $d_p = 0$ ; Block thickness: (□) 5 mm; (Δ) 10 mm; (○) 20 mm. The combined curves (addition of the two curves) are represented by black symbols. Block thickness: (■) 5 mm; (▲) 10 mm; (●) 20 mm. (b)  $d_p = 10 \mu\text{m}$ ; Block thickness: (□) 5 mm; (Δ) 10 mm; (○) 20 mm. The combined curves (addition of the two curves) are represented by black symbols. Block thickness: (■) 5 mm; (▲) 10 mm; (●) 20 mm.

thickness that has to be resorbed in order to resorb one unit cell of the block,  $th_{r,tot}$  (Fig. 1) depends obviously on the geometry of the unit cell, in the present case the CFC lattice (Fig. 1). In this lattice, the largest distance between two neighboring pores corresponds to the diameter,  $d_{octgap}$ , of the octahedral gap present within the lattice (Fig. 1b). This diameter is

$$d_{octgap} = 2r_p(\sqrt{2} - 1) + d_p(\sqrt{2}). \quad (22)$$

Therefore, the layer thickness that has to be resorbed in order to fully resorb one unit cell corresponds to half of this distance, i.e.

$$th_{r,tot} = \frac{d_{octgap}}{2} = r_p(\sqrt{2} - 1) + d_p \left( \frac{\sqrt{2}}{2} \right). \quad (23)$$

The results show that the latter radius increases linearly with an increase of the pore radius (Fig. 13). The total layer thickness that has to be resorbed in order to

fully resorb the ceramic is then defined by the addition of the results of Eqs. (21) and (23) (Fig. 13)

$$th_{tot} = r_p(\sqrt{2} - 1) + d_p \left( \frac{\sqrt{2}}{2} \right) + \frac{\sqrt{r_i^2 + (2r_p + d_p - \sqrt{r_p^2 - r_i^2})^2} - r_p}{4r_p + 2d_p} W \quad (24)$$

for  $d_p > -2(r_p - \sqrt{r_p^2 - r_i^2})$ .

As the resorption time is proportional to the total layer thickness that has to be resorbed in order to fully resorb the ceramic, a minimum in the maximum resorption time is observed at various pore sizes depending on the block size and the inter-pore distance,  $d_p$ . For example, for  $d_p = 0$ , the minimum is seen in the radius range of 150–250 μm (Fig. 13a). For a slightly larger  $d_p$  value ( $d_p = 10 \mu\text{m}$ ), the range is moved to larger values, i.e. in the range of 200–400 μm (Fig. 13b). For  $d_p = 30 \mu\text{m}$  (not shown here), this range is seen at even larger radii (from 300 to 600 μm). For  $d_p$  values negative enough to have  $r_i > 25 \mu\text{m}$  (Eq. (12)), bone ingrowth is not limited by the presence of closed interconnections, but by the time required to resorb one unit cell. In that case, the optimal pore radius is lower than the optimal range found for  $d_p = 0$  (150–250 μm) but also higher than the minimum size  $r_i = 25 \mu\text{m}$ . At low radii, the porosity of fully open blocks is indeed so high (Fig. 7) that the blocks are mechanically too weak. Therefore, a trade-off between fast bone ingrowth, resorption rate, and porosity has to be found. A pore radius superior to 100 μm seem to be a good choice.

### 2.2. Convex bone substitutes

The resorption rate of ceramic bone substitutes does not only depend on their porosity, but also on their shape and size. Assuming that the resorption rate takes place via surface mechanisms, the resorption rate in the cross-section of ceramic bone substitutes becomes a linear function of the bone substitute thickness. For example, the radius of a spherical granule varies according to

$$r_{g,t} = r_{g,0} - R_R t, \quad (25)$$

where  $R_R$  is the linear resorption rate,  $r_{g,0}$  and  $r_{g,t}$  are the radius at time 0 and  $t$ , respectively. Therefore, a twofold increase of the granule size leads to a twofold increase of the resorption time,  $t_r$ . However, the evolution of the volume of the granule is not a linear function of time (Fig. 14a)

$$V_{g,t} = V_{g,0} \left( 1 - \frac{R_R}{r_{g,0}} t \right)^3, \quad (26)$$

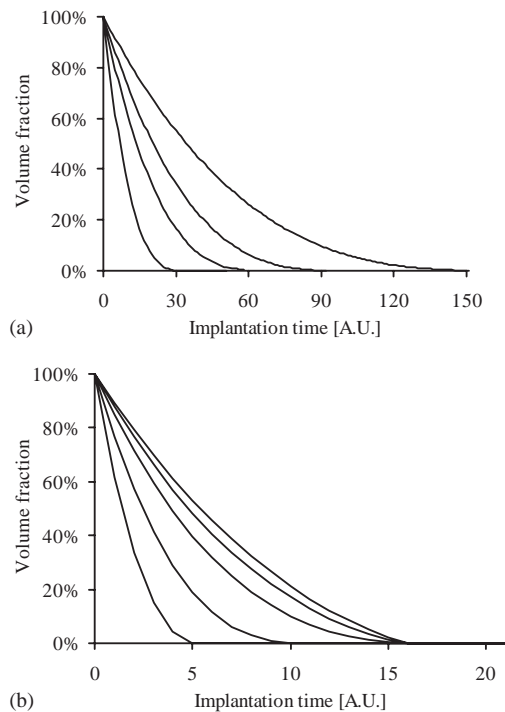


Fig. 14. Evolution as a function of time of the volume fraction of (a) spherical granules and (b) cylinders. For granules, four cases are represented corresponding to a granule radius of:  $r_g = 1, 2, 3,$  and  $5$  (from left to right). For cylinders, five cases are represented corresponding to a cylinder radius of:  $r_c = 2, 4, 8, 12$  and  $16$ . Height:  $12$ . The granule radius and the implantation time are in arbitrary units.

where  $V_{g,0}$  and  $V_{g,t}$  are the volume at time 0 and  $t$ , respectively. A similar expression can be calculated for cylinders (Fig. 14b)

$$V_{cyl,t} = V_{cyl,0} \left(1 - \frac{R_R}{r_{cyl,0}} t\right)^2 \left(1 - 2 \frac{R_R}{h_{cyl,0}} t\right), \quad (27)$$

where  $V_{cyl,0}$  and  $V_{cyl,t}$  are the volume at time 0 and  $t$ , respectively, and  $r_{cyl,0}$  and  $h_{cyl,0}$  are the initial radius and height. Interestingly, the shape of the resorption curve varies with the ratio between the height and the radius of the cylinder. For blocks or flat wedges, a similar expression can be calculated

$$V_{prism,t} = V_{prism,0} \left(1 - \frac{R_R}{l_{prism,0}} t\right) \left(1 - \frac{R_R}{w_{prism,0}} t\right) \times \left(1 - \frac{R_R}{h_{prism,0}} t\right). \quad (28)$$

Interestingly, the volume resorption rate is almost linear if one of the dimensions is much smaller than the two other ones (e.g.  $h_{prism,0} \ll l_{prism,0}$  and  $w_{prism,0}$ ).

### 2.3. Conclusion of the theoretical part

In conclusion, it appears that a fast resorption rate of bone substitutes can only be reached if the bone

substitutes possess an optimum surface area and allow a fast bone ingrowth. This criterion can be met but the solution differs between concave and convex bone substitute.

#### 2.3.1. Concave bone substitute

*Open structures:* The best would be to have a fully open porous structure (interconnection diameter:  $50 \mu\text{m}$ ) with a diameter hardly larger than  $50 \mu\text{m}$  in diameter. Unfortunately, such a structure would be extremely brittle due to its very high porosity (Fig. 7). Therefore, a trade-off between resorption rate and mechanical property has to be found. A pore radius superior to  $100 \mu\text{m}$  seems to be a good choice. Interestingly, the pore size optimum of a fully open bone substitute does not depend on the size of the bone substitute.

*Closed structures:* In practice, it is difficult to synthesize a fully open-porous ceramic bone substitute. Therefore, the large majority of synthetic bone substitutes have only a partially open structure. In that case, the optimal pore radius is a function of the block size and the interpore distance (Fig. 13). Typical values were found in the range of  $150\text{--}400 \mu\text{m}$  (Fig. 13). Therefore, in vivo experiments conducted on closed or only partially open porous structures might give different results (in terms of an optimum pore diameter) depending on the geometry and the size of the porous bone substitute. Moreover, relatively large pores do not have to be interconnected to lead to a fast implant resorption (Fig. 10).

#### 2.3.2. Convex bone substitute

When the bone substitute does not contain macropores, it is important to reduce the size of the bone substitute to increase the resorption rate (Fig. 14). Typical radii should probably be around  $100\text{--}200 \mu\text{m}$  to achieve a good balance between a high surface area (with a small particle size) and the presence of sufficiently large gaps between the particles (with a large particle size). It might be adequate also to have an irregular shape that can on one side increase the specific surface area and on the other side increase the size of the gaps between particles.

### 2.4. Limitations of the model

All the latter conclusions are based on theoretical calculations and simple assumptions, the goal being to maximize bone resorption. Like any other model, the present model has limitations. Two types of limitations linked to two questions can be raised: (i) How adequate are the assumptions of the model? (ii) Are there other aspects that have not been considered in the model that could have a large effect?

### 2.4.1. Adequacy of the assumptions

As initially mentioned, five assumptions were included in the model: (i) the pores are spherical; (ii) the pores are ordered according to a face-centered cubic packing; (iii) the resorption is surface-controlled; (iv) the resorption is only possible if the surface can be accessed by blood vessels of 50  $\mu\text{m}$  in diameter; and (v) the resorption time of a given amount of calcium phosphate is proportional to the net amount of material.

The first assumption is based on the observation that many bone substitutes contain spherical or almost spherical pores that are characterized by an aspect ratio close to 1. It is indeed easier to produce bone substitutes with such pores than with pores presenting a large aspect ratio. It is also easier to mathematically describe their resorption. However, it is clear that other geometries might be preferred. For example, an optimal bone substitute would probably have fully interconnected cylindrical pores with a diameter close to 50  $\mu\text{m}$ . But as previously mentioned, this study is devoted to bone substitutes having spherical or almost spherical macropores.

The second assumption is again a clear approximation of the reality, but it is easier to assume such a pore distribution than to assume a random distribution of the pores. In the latter case, a finite element approach would have had to be used, which is much more cumbersome. In a CFC structure, all pores are equidistantly distributed. This means that the diameters of the pore interconnections are minimized whereas the maximum solid distance within the bone substitute is minimized. If the pores were randomly distributed, larger pore interconnections and larger solid distances would be found. In other words, less resorption would be required to open up the structure (i.e. less than the prediction of Eq. (21)), but more resorption would be required to resorb a unit cell (i.e. more than the prediction of Eq. (23)). As a result, the optimum pore radius of a randomly distributed pore structure (in terms of ceramic resorption) would be decreased compared to a CFC pore distribution. However, there would still be an optimum of pore size and there would still be an effect of bone substitute size on the optimum pore size. So, a change of the first assumption would not markedly modify the conclusions of the model.

The third assumption is based on the fact that traditional calcium phosphate compounds, such as  $\beta$ -tricalcium phosphate and hydroxyapatite, are mainly resorbed by osteoclasts and/or macrophages which are located at or in close vicinity of the ceramic surface [9]. One important question that can be raised is whether the calcium and phosphate ions released by osteoclasts and macrophages can interact with the activity of neighboring osteoclasts and macrophages. It is likely that a too large resorption rate leads to a poor biocompatibility due to high concentrations of calcium and phosphate

ions in the microenvironment around the bone substitutes, possibly leading to an acute or chronic inflammatory response [1]. If it is really the case, the model should be modified. However, these modifications cannot be made because it is not known how osteoclasts and macrophages interact together. So the third assumption is taken as a first approximation.

Cells can only survive in the close vicinity of blood vessels. It is therefore a prerequisite to have blood vessels within a macroporous ceramic in order to have cellular resorption. According to Lu et al. [8], a minimum pore interconnection diameter of 50  $\mu\text{m}$  is sufficient. Other values have been mentioned by other authors, for example 100  $\mu\text{m}$ . An increase of the interconnection diameter from 50 to 100  $\mu\text{m}$  in the model would not modify the time required to resorb a unit cell (Eq. (23)) but increase the time required to open the structure in order to enable bone ingrowth (Eq. (21)). As a result, a small increase of the optimum pore size would be measured.

The fifth hypothesis is based on the fact that the amount of acid required to dissolve a given calcium phosphate bone substitute is proportional to the amount of material (keeping the same chemistry).

### 2.4.2. Other aspects likely to influence the *in vivo* response

In practical applications, other aspects must be considered which might limit the validity and accuracy of the model. For example, the model only considers one resorption pathway, i.e. the physicochemical dissolution of the calcium phosphate at the implant surface. Several studies assume that the resorption can also proceed by desintegration of the material into small particles and subsequent intracellular digestion or transportation to neighboring tissues such as lymph nodes [10,11]. This is in particular true for microporous calcium phosphate materials [10–13]. In that regard, it seems that microporous materials are resorbed faster than macroporous materials [14], because of the possibility for the body to resorb the material via several pathways, i.e. osteoclasts, macrophages and lymph nodes. However, more data would be needed to confirm this hypothesis. In any case, to include this additional resorption pathway in the model would not modify the conclusions of the model.

The model also assumes that blood vessels and cells move instantaneously into the bone substitute provided a path with a diameter superior to 50  $\mu\text{m}$  is present. This assumption is certainly not correct, especially for fast resorbing calcium phosphate materials. In that case, a new term should be included in the model besides the time required to open up the structure (Eq. (21)) and the time required to resorb one unit cell (Eq. (23)). This new term would describe the time required by cells and blood vessels to move into the structure. It is expected that this time is almost independent of the pore size, but increases

with an increase of the block size. As a result, a slow blood vessel ingrowth and cell migration should favor small pore size optima.

A third limitation of the model is the fact that it does not take into account possible chemical changes of the implant. For example, brushite cements are known to be transformed into apatite over time [15,16], which leads to a strong reduction of the resorption rate. To limit this effect, it is probably important to have a highly open structure that promotes a good exchange of body fluids.

In the present model, it was assumed that the resorption rate was independent of the extent of resorption. In fact, some authors [10,17] report that the resorption of calcium phosphate ceramics proceeds faster at early implantation times than at later times. Therefore, it appears that in order to minimize the total resorption time of the ceramic, resorbing cells should have access to the pore surface area as fast as possible. If the bone substitute can be freely invaded by resorbing cells, a small pore size appears to be the most adequate. If the bone substitute cannot be freely colonized by cells, larger pores should be preferred because less resorption is required to fully open the structure (Eq. (23); Fig. 13).

It is well-known that  $\beta$ -tricalcium phosphate does not resorb as slowly as hydroxyapatite even though both ceramics are resorbed by osteoclasts and macrophages. This is due to differences in solubility. However, to relate the calcium phosphate chemistry to the resorption rate is a very complicated matter. Therefore, no attempt was made to propose a relationship between resorption rate and solubility. Nevertheless, the effect of calcium phosphate chemistry was included indirectly in the model via the linear resorption rate,  $R_R$ . This value is adjusted when experimental results are fitted with the model (see hereafter).

Summarizing this section, it can be stated that the present model is similar to any model, i.e. it provides predictions based on assumptions that simplify the investigated system. The evaluation of the effect of these simplifications and assumptions shows that some of those simplifications and assumptions favors smaller pore sizes, whereas other favor larger pore sizes. In conclusion, the only way to assess the adequacy of the model is to compare the predictions of the model with experimental results. This is the goal of the following paragraph.

### 3. Experimental results

Generally, there is very little data available in the literature to assess the adequacy of the present model. Very few studies investigated the biological response at three or more implantation times. Moreover, the extent of bone ingrowth and calcium phosphate resorption was in most cases not determined. Finally, not all results are

reliable. The reason stems from the difficulties associated with histomorphometrical measurements. For example, Dupraz et al. [18] attempted to measure the resorption of granules over time. These authors chose to determine the total surface area of the granules in a histological cut. However, granules can move over time, for example by sedimentation. This can probably explain why the residual granule surface area continuously increased and decreased over time. An alternative method would be to measure the radius of the particles over time. But if the granules are not perfectly spherical (as in [18]) and if a few hundreds of granules are present in one section, such a method would become rapidly very cumbersome. Another example is the study of Ohura et al. [3] who investigated the resorption rate of one particular brushite cement. The determination of the residual cement amount was made radiographically. The latter method can only give a crude approximation of the residual cement because it can not well discriminate between calcium phosphate and bone.

Another difficulty to correlate the present model with published experimental data stems from the difficulties related to the synthesis of calcium phosphate bone substitutes with perfectly controlled geometry. It is indeed very difficult to synthesize a range of blocks or granules where only one parameter varies, e.g. where the interconnection size varies but where the pore size stays constant; or to synthesize round granules and to vary their size without varying their apparent density. Recent works show how porous blocks can be synthesized with a well-controlled pore size and interconnection size [19,20]. Additionally, monosized granules of high sphericity can be now produced. These new techniques have started being used [21], and will allow to gain a better understanding of the resorption of bone substitutes.

#### 3.1. Concave bone substitutes (macroporous blocks)

As mentioned for CPC, there is also very little data available on the biological behavior of blocks with various porosities (Table 1). Gauthier et al. [22] studied porous blocks of biphasic calcium phosphate. Four different blocks corresponding to two different porosities (40% and 50%) and two different pore diameters (300 and 565  $\mu\text{m}$ ) were investigated. There was significantly more bone in the 565  $\mu\text{m}$  pore blocks than in the 300  $\mu\text{m}$  pore blocks, apparently independently of the porosity. This conclusion is in agreement with the theoretical results showing that for the same porosity, faster bone ingrowth and more bone formation should be measured in blocks with larger pores (Fig. 13). Other authors such as Uchida et al. (pore diameters: 210–300  $\mu\text{m}$  and 150–210  $\mu\text{m}$ ; [23]), Kuhne et al. (pore diameters: 500 and 200  $\mu\text{m}$ ; [24]), and Shimazaki and Mooney (pore diameters: 600 and 230  $\mu\text{m}$ ; [25]) ob-

Table 1

Summary of the experimental data found in the literature and their best fit. As the different materials with different micro- and nanoporosities were used, the linear resorption rate,  $R_R$ , was fitted in each case

Article	Defect type	Histological section	Calcium phosphate	Time periods	Correlation coefficient ( $r^2$ )
[29]	Cylinder	Cross-section	Apatite cement	2, 8, 16, 24 w	0.93
[30]	Cylinder	Cross-section	Apatite cement	2, 4, 8, 16, 32, 78 w	0.99
[33]	Cylinder	Cross-section	Apatite cement	2, 4, 8, 12, 24 w	0.77
[27]	Cylinder	Cross-section	Brushite cement	2, 4, 12, 24 w	0.98
[15,28]	Cylinder	Cross-section	Brushite cement	2, 4, 6, 8 w	0.99
[34]	Cylinder	Cross-section	Brushite cement	2, 6, 18 w	0.99
[3]	Cylinder	Longitudinal section	Brushite cement A	4, 8, 16 w	0.999
[3]	Cylinder	Longitudinal section	Brushite cement B	4, 8, 16 w	1.00
[26]	Cylinders	Cross-section	$\beta$ -TCP	2 w, 4 w, 4 m, 6 m	0.97
[18]	Granules	Section	BCP	1, 4, 12, 26, 52, 78 w	0.49
[11]	Granules	Section	$\beta$ -TCP	2, 4, 8, 16, 32 d	0.97
[30]	Wedge	Cross-section	Apatite cement	2, 4, 8, 16, 78 w	0.81

served similar results. Egli et al. [26] implanted  $\beta$ -TCP and HA blocks of two different pore diameters (50–100 and 200–400  $\mu\text{m}$ ) in rabbits during 2 weeks, 4 weeks, 4 months and 6 months. These authors observed a faster resorption of the blocks with the smaller pore size, in disagreement with the present model. Additionally, Egli et al. [26] and Grynypas et al. [17] observed a faster bone ingrowth with small pores, again in disagreement with the present model. The proposed explanation was the following: “smaller pores expose a much larger surface to the invading tissue elements and thus favor deposition”.

In his paper, Lu et al. [8] mentioned that “in resorbable materials, pore and interconnection densities play a more important role than their size, because sizes are modified by degradation”. The present model contradicts this statement because the resorption of larger pores modifies more effectively the size of pore interconnections than the resorption of small pores (Fig. 9). The same authors mention that “interconnections act only as pathways for nutritional elements, vascularization and cells, although pores are the sites for bone tissue growth. Thus pore size must be larger than interconnection size”. This statement would mean that pores cannot be simply tubular as proposed herein when discussing an ideal block porosity.

### 3.2. Convex bone substitutes

#### 3.2.1. Calcium phosphate cements

Despite an increasing interest for these materials, there is little data in the literature relative to the resorption rate of calcium phosphate cements (CPC). CPC are characterized by a relatively large microporosity (40–60%) and the absence of macroporosity that enable bone ingrowth (Fig. 7). As a result, the resorption proceeds layer by layer. Some researchers have attempted to quantify the resorption rate of CPC over time [3,27–30]. Most studies have been done with

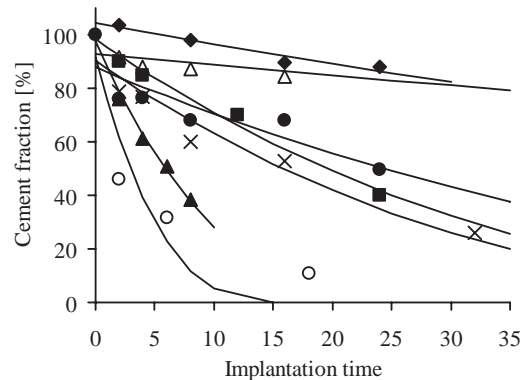


Fig. 15. Evolution of the volume fraction of cylinders and granules as a function of time. The symbols represent the results obtained in vivo. ( $\blacktriangle$ ) (Theiss et al.); ( $\blacksquare$ ) Lu et al. [22]; ( $\triangle$ ) Frankenburg et al. [25]; ( $\times$ ) Koerten and van der Meulen [11]; ( $\blacklozenge$ ) Ooms et al. [24]; ( $\circ$ ) Frayssinet et al. [35]; ( $\bullet$ ) Oberle et al. [34]. The curves are the best fits of the data.

cylinders. These experimental results and theoretical curves demonstrate a very good agreement (Table 1, Figs. 15 and 16), suggesting that the simple theoretical model is useful. In apatite CPC, where apatite is the end-product of the reaction, the resorption rate is very slow [29,30]. Therefore, very small variations of the resorbed amount are measured over time. Additionally, these cements are often difficult to inject, which might lead to imperfect defect filling. It is therefore difficult to get data over an adequate time range i.e. from 0% to 60–80% resorption as for Theiss et al. [28]. For example, Ooms et al. [29] measured only 20% resorption after 24 weeks. Frankenburg et al. [30] studied another apatite cement where the resorbed amount reached about 20% at 16 weeks, and almost 70% at 78 weeks. The results of Ohura et al. [3] were difficult to analyze because only three implantation times were studied, and because the resorbed cement fraction at the last time point was close to zero (<1%). Table 1 gives the summary of all the experimental fits. It appears that the correlation

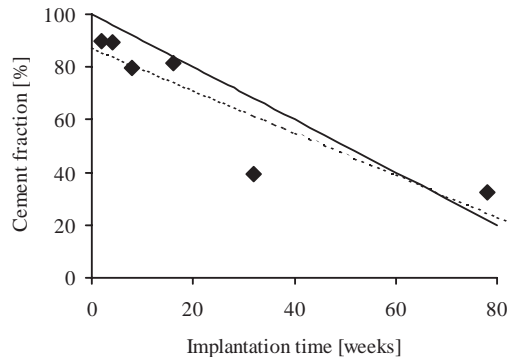


Fig. 16. Evolution of the volume fraction of wedges as a function of time (line). The symbols represent the results obtained with calcium phosphate cement wedges in vivo. (◆) Frankenburg et al. [25]. The dotted line represents the fit of the data of Frankenburg et al assuming that initially the defect was not fully filled with the cement.

coefficient,  $r^2$ , obtained by fitting the experimental data with the model is in all but one case larger than 0.8.

### 3.2.2. Granules

Another interesting case is represented by granules. If the resorption rate is surface controlled, the volume fraction decreases with time (Fig. 14). Additionally, the rate of resorption decreases with time (slope of the curve in Fig. 14). Moreover, the time required to complete the resorption is inversely proportional to the granule size. Therefore, a fivefold increase of the granule diameter leads to a fivefold increase of the resorption time. Experimentally, Gauthier et al. [31] observed that the resorption of biphasic calcium phosphate granules proceeded faster with a diameter of 40–80  $\mu\text{m}$  than with a diameter of 200–500  $\mu\text{m}$ . Additionally, the resorption rate decreased with implantation time: at 2 weeks, the resorption rate was twice larger than at 8 weeks. Both observations confirm the predictions of the model.

In another study, Malard et al. [32] compared the resorption rate of BCP granules with three different particle diameters, i.e. 10–20, 80–100, and 200–400  $\mu\text{m}$ . Again, a strong decrease of the activity of multinucleated giant cells was observed over time (between day 7 and day 14). Moreover, the BCP surface area decreased significantly from day 7 to day 21. Finally, the BCP surface area was significantly smaller in the 10–20  $\mu\text{m}$  range 14 and 21 days after implantation than in the 80–100  $\mu\text{m}$  ( $p < 0.05$ ) and 200–400  $\mu\text{m}$  ( $p < 0.01$ ) ranges.

Dupraz et al. [18] investigated the resorption of ceramic granules as a function of time. The granules had a diameter in the range of 80–200  $\mu\text{m}$ . Unfortunately, increases and decreases of the ceramic fraction were observed with time, suggesting that some granules had moved away from the defect and that the authors had perhaps also difficulties to spot the location of the granules.

Grynepas et al. [17] implanted rods of calcium pyrophosphate ( $\text{Ca}_2\text{P}_2\text{O}_7$ ) in the distal femur of rabbits. These blocks were constituted of small particles sintered together. The porosity of the blocks was kept constant at 60%, while the sintered particles had three different diameters: 45–105, 105–150, and 150–250  $\mu\text{m}$ . The results showed that the resorption rate was inversely proportional to the size of the particles. For example, at 6 weeks, the volume fraction of the block decreased from 62% to 33% with the 45–105  $\mu\text{m}$  particles, from 59% to 43% with the 105–150  $\mu\text{m}$  particles and from 58% to 53% with the 150–250  $\mu\text{m}$  particles. Using the present model, the resorption rate  $R_R$  of the granules can be estimated for each particle size. The results are 1.2, 1.1 and 0.5  $\mu\text{m}/\text{week}$  for the particle diameters 45–105  $\mu\text{m}$  (average 75  $\mu\text{m}$ ), 105–150  $\mu\text{m}$  (average 127  $\mu\text{m}$ ), and 150–250  $\mu\text{m}$  (average 200  $\mu\text{m}$ ). Therefore, the granules should disappear in 32, 56 and 203 weeks, respectively. However, the volume fraction of the block made with the 45–105  $\mu\text{m}$  particles decreased from 62% at time zero to 33% at 6 weeks and to 27% at 1 year. For the 105–150  $\mu\text{m}$  particles, these values were: 59% at time zero, 43% at 6 weeks, and 39% at 1 year. Therefore, experimental results suggest that the linear resorption rate of ceramic material decreases with the implantation time. In the present model, it was assumed that the resorption rate was constant. This difference could explain the small discrepancies observed between model and experimental results (Table 1).

## 4. Conclusions

The resorption model presented in this study predicts that the time required to fully resorb a macroporous bone substitute (= concave bone substitute) depends on two factors: (i) the time required to fully open the structure and (ii) the time required to resorb one unit cell. The first factor decreases almost exponentially with an increase of pore size, whereas the second factor increases linearly with the same pore size. So, if the structure is already fully open before implantation, the optimal pore diameter should be close to 50  $\mu\text{m}$ . However, as such a structure would be very porous and hence very brittle, a pore size superior to 100  $\mu\text{m}$  appears more appropriate. If the bone substitute is initially not fully open, a minimum of resorption time is found at an intermediate pore size. Unfortunately, this value is not unique, but increases with an increase of the interpore distance and more importantly with an increase of the bone substitute size. Pore radii in the range of 150–400  $\mu\text{m}$  were calculated. These values are similar to the values found in in vivo studies. For dense or microporous blocks (convex bone substitutes), the resorption time only depends on the resorption rate of the outer surface. Therefore, a small external granule

diameter should be preferred, but it should not be too small because bone ingrowth between the granules would be prevented. Typical radii should probably be around 100–200  $\mu\text{m}$ . The comparison of the model predictions with experimental data shows a very good agreement, i.e. in most cases, more than 80% of the results can be explained with the model. However, the present model overestimates the resorption rate at late implantation times, possibly because of the inflammatory reactions present in the first weeks after surgery and/or the formation of a protective bone layer on the ceramic surface at later times. Nevertheless, the model appears to be a useful tool to better understand in vivo results, and to define more adequate geometries for bone substitutes.

## References

- [1] Jarcho M. Phosphate ceramics as hard tissue prosthetics. *Clin Orthop Relat Res* 1981;157:259–78.
- [2] Munting E, Mirtchi AA, Lemaître J. Bone repair of defects filled with phosphocalcic hydraulic cement: an in vivo study. *J Mater Sci Mater Med* 1993;4:337–44.
- [3] Ohura K, Bohner M, Hardouin P, Lemaître J, Pasquier G, Flautre B. Resorption of, and bone formation from, new beta-tricalcium phosphate-monocalcium phosphate cements: an in vivo study. *J Biomed Mater Res* 1996;30(2):193–200.
- [4] Kamakura S, Sasano Y, Nakajo S, Shimizu T, Suzuki O, Katou F, Kagayama M, Motegi K. Implantation of octacalcium phosphate combined with transforming growth factor-beta1 enhances bone repair as well as resorption of the implant in rat skull defects. *J Biomed Mater Res* 2001;57(2):175–82.
- [5] Kamakura S, Sasano Y, Shimizu T, Hatori K, Suzuki O, Kagayama M, Motegi K. Implanted octacalcium phosphate is more resorbable than beta-tricalcium phosphate and hydroxyapatite. *J Biomed Mater Res* 2002;59(1):29–34.
- [6] Knabe C, Driessens FC, Planell JA, Gildenhaar R, Berger G, Reif D, Fitzner R, Radlanski RJ, Gross U. Evaluation of calcium phosphates and experimental calcium phosphate bone cements using osteogenic cultures. *J Biomed Mater Res* 2000;52(3):498–508.
- [7] Lin FH, Liao CJ, Chen KS, Sun JS, Liu HC. Degradation behaviour of a new bioceramic:  $\text{Ca}_2\text{P}_2\text{O}_7$  with addition of  $\text{Na}_4\text{P}_2\text{O}_7 \cdot 10\text{H}_2\text{O}$ . *Biomaterials* 1997;18(13):915–21.
- [8] Lu JX, Flautre B, Anselme K, Hardouin P, Gallur A, Descamps M, Thierry B. Role of interconnections in porous bioceramics on bone recolonization in vitro and in vivo. *J Mater Sci Mater Med* 1999;10:111–20.
- [9] Mostov K, Werb Z. Journey across the osteoclast. *Science* 1997;276:219–20.
- [10] de Groot K. Effect of porosity and physicochemical properties on the stability, resorption, and strength of calcium phosphate ceramics. *Ann N Y Acad Sci* 1988;523:227–33.
- [11] Koerten HK, van der Meulen J. Degradation of calcium phosphate ceramics. *J Biomed Mater Res* 1999;44:78–86.
- [12] Klein CPAT, Driessens AA, de Groot K. Relationship between the degradation behaviour of calcium phosphate ceramics and their physical–chemical characteristics and ultrastructural geometry. *Biomaterials* 1984;5:157–60.
- [13] Klein CPAT, de Groot K, Driessens AA, van der Lube HBM. Interaction of biodegradable  $\beta$ -whitlockite ceramics in bone tissue: an in vivo study. *Biomaterials* 1985;6:189–92.
- [14] Ioku K, Goto S, Kurosawa H, Shibuya K, Yokozeki H, Hayashi T, Nakagawa T. Reaction of porous  $\beta$ -TCP with different microstructure in vivo. *Bioceramics* 1995;9:201–4.
- [15] Bohner M, Theiss F, Apelt D, Hirsiger W, Houriet R, Rizzoli G, Gnos E, Frei C, Auer JA, von Rechenberg B. Compositional changes of a dicalcium phosphate dihydrate cement after implantation in sheep. *Biomaterials* 2003;24(20):3463–74.
- [16] Penel G, Leroy N, Van Landuyt P, Flautre B, Hardouin P, Lemaître J, Leroy G. Raman microspectrometry studies of brushite cement: in vivo evolution in a sheep model. *Bone* 1999;25S(2):81–4.
- [17] Grynepas MD, Pilliar RM, Kandel RA, Renlund R, Filiaggi M, Dumitriu M. Porous calcium polyphosphate scaffolds for bone substitute applications in vivo studies. *Biomaterials* 2002;23:2063–70.
- [18] Dupraz A, Delecrin J, Moreau A, Pilet P, Passuti N. Long-term bone response to particulate injectable ceramic. *J Biomed Mater Res* 1998;42(3):368–75.
- [19] Richart O, Descamps M, Liebetrau A. Macroporous calcium phosphate ceramics: optimization of the porous structure and its effects on the bone ingrowth in a sheep model. *Key Eng Mater* 2001;192–195:425–8.
- [20] Richart O, Descamps M, Liebetrau A. Preparation and mechanical characterization of hydroxyapatite monodispersed macroporous structure. Influence of interconnection and macropores diameters. *Key Eng Mater* 2002;218–220:9–12.
- [21] Lu JX, Gallur A, Flautre B, Anselme K, Descamps M, Thierry B, Hardouin P. Comparative study of tissue reactions to calcium phosphate ceramics among cancellous, cortical, and medullar bone sites in rabbits. *J Biomed Mater Res* 1998;42(3):357–67.
- [22] Gauthier O, Bouler J-M, Aguado E, Pilet P, Daculsi G. Macroporous biphasic calcium phosphate ceramic: influence of macropore diameter and macroporosity percentage on bone ingrowth. *Biomaterials* 1998;19:133–9.
- [23] Uchida A, Nade SM, McCartney ER, Ching W. The use of ceramics for bone replacement. A comparative study of three different porous ceramics. *J Bone Joint Surg Br* 1984;66(2):269–75.
- [24] Kuhne JH, Bartl R, Frisch B, Hammer C, Jansson V, Zimmer M. Bone formation in coralline hydroxyapatite. Effects of pore size studied in rabbits. *Acta Orthop Scand* 1994;65(3):246–52.
- [25] Shimazaki K, Mooney V. Comparative study of porous hydroxyapatite and tricalcium phosphate as bone substitute. *J Orthop Res* 1985;3(3):301–10.
- [26] Egli PS, Mueller W, Schenk RK. Porous hydroxyapatite and tricalcium phosphate cylinders with two different pore size ranges implanted in the cancellous bone of rabbits. *Clin Orthop* 1988;232:127–38.
- [27] Lu JX, About I, Stephan G, Van Landuyt P, Dejou J, Fiochi M, Lemaître J, Proust JP. Histological and biomechanical studies of two bone colonizable cements in rabbits. *Bone* 1999;25S(2):41–5.
- [28] Theiss F, Apelt D, Brand B, Bohner M, Frei C, Auer JA, von Rechenberg B. Biocompatibility and resorption of a new brushite calcium phosphate cement. *Biomaterials*, submitted for publication.
- [29] Ooms EM, Wolke JG, van der Waerden JP, Jansen JA. Trabecular bone response to injectable calcium phosphate (Ca-P) cement. *J Biomed Mater Res* 2002;61(1):9–18.
- [30] Frankenburg EP, Goldstein SA, Bauer TW, Harris SA, Poser RD. Biomechanical and histological evaluation of a calcium phosphate cement. *J Bone Joint Surg Am* 1998;80(8):1212–24.
- [31] Gauthier O, Bouler J-M, Weiss P, Bosco J, Daculsi G, Aguado E. Kinetic study of bone ingrowth and ceramic

- resorption associated with the implantation of different injectable calcium-phosphate bone substitutes. *J Biomed Mater Res* 1999; 47:28–35.
- [32] Malard O, Bouler J-M, Guicheux J, Heymann D, Pilet P, Coquard C, Daculsi G. Influence of biphasic calcium phosphate granulometry on bone ingrowth, ceramic resorption, and inflammatory reactions: preliminary in vitro and in vivo study. *J Biomed Mater Res* 1999;46:103–11.
- [33] Oberle A, Theiss F, Böhner M, Mueller J, Frei C, Boecken I, Zlinsky K, Auer JA, von Rechenberg B. Vergleich eines neuartigen Brushite-Kalzium phosphat-Zement mit einem herkömmlichen Hydroxylapatit-Kalziumphosphat-Zement in vivo. *Der Orthopäde*, submitted for publication.
- [34] Frayssinet P, Gineste L, Conte P, Fages J, Rouquet N. Short-term implantation effects of a DCPD-based calcium phosphate cement. *Biomaterials* 1998;19:971–8.